Pacific Northwest
NATIONAL LABORATORY

Proudly Operated by **Battelle** *Since 1965*

Concept Feasibility Report for Electroplating Zirconium onto Uranium Foil

March 2015

GW Coffey   LR Pederson
KD Meinhardt   CA Lavender
VV Joshi   DE Burkes

DISCLAIMER

This report was prepared as an account of work sponsored by an agency of the United States Government. Neither the United States Government nor any agency thereof, nor Battelle Memorial Institute, nor any of their employees, makes **any warranty, express or implied, or assumes any legal liability or responsibility for the accuracy, completeness, or usefulness of any information, apparatus, product, or process disclosed, or represents that its use would not infringe privately owned rights**. Reference herein to any specific commercial product, process, or service by trade name, trademark, manufacturer, or otherwise does not necessarily constitute or imply its endorsement, recommendation, or favoring by the United States Government or any agency thereof, or Battelle Memorial Institute. The views and opinions of authors expressed herein do not necessarily state or reflect those of the United States Government or any agency thereof.

This document was printed on recycled paper.
(8/2010)

Concept Feasibility Report for Electroplating Zirconium onto Uranium Foil

GW Coffey   LR Pederson
KD Meinhardt   CA Lavender
VV Joshi   DE Burkes

March 2015

Pacific Northwest National Laboratory
Richland, Washington 99352

Summary

The Fuel Fabrication Capability of the U.S. High Performance Research Reactor Conversion Program is funded through the National Nuclear Security Administration NA-23 (Office of Material Management and Minimization). It commissioned an investigation to determine the feasibility of using electroplating techniques to apply a coating of zirconium on depleted uranium-10 wt% molybdenum alloy (U-10Mo). Electroplating would provide an alternative method to the existing process of hot-roll bonding zirconium foil onto the U-10Mo fuel foil during the fabrication of fuel elements for high-performance research reactors. The objective of this research was to develop a reproducible and scalable plating process that will produce a uniform, 25 μm thick, zirconium metal coating on U-10Mo foil.

In the initial phase of this work, Pacific Northwest National Laboratory (PNNL) established a molten salt electroplating apparatus and protocol to plate zirconium metal onto molybdenum foil. During the second phase of the research reported herein, PNNL furthered this work by moving to the U-10Mo. The original plating apparatus was disassembled and re-assembled in a laboratory capable of handling low-level radioactive materials. Initially, the work followed the previous "Zr onto Mo plating" protocol where the salt bath composition was targeted at the eutectic composition (LiF:NaF:ZrF_4 = 26:37:37 mol%). Early results indicated that the formation of uranium fluoride compounds would be problematic. Other salt bath compositions were investigated to eliminate the uranium fluoride production (LiF:NaF = 61:39 mol% and LiF:NaF:KF = 46.5:11.5:42 mol%). Zirconium metal was used as the crucible for the molten salt. Three plating methods were used—isopotential, galvano static, and pulsed plating.

The molten salt method for zirconium metal application provided high-quality plating on molybdenum in PNNL's previous work. A key advantage of this approach is that plating can be performed under conditions that would greatly reduce the quantity of intermetallics that form at the interface between the zirconium and U-10Mo; unlike roll bonding, the molten salt plating approach allows for complete coverage of the U-10Mo foil with zirconium. When using the experimental parameters developed for zirconium plating onto molybdenum, a uranium fluoride reaction product was formed at the Zr/U-10Mo interface. By controlling the initial plating potential, the uranium fluoride could be prevented; however, the targeted zirconium thickness (25 ±12.5 μm) could not be achieved while maintaining 100% coverage.

Acronyms and Abbreviations

amp	ampere(s)
°C	degrees Celsius
cm	centimeter(s)
cm^2	square centimeter(s)
CV	cyclic voltammetry
DC	direct current
FFC	Fuel Fabrication Capability
ft	foot(feet)
HEU	highly enriched uranium
HF	hydrofluoric acid
KF	potassium fluoride
LEU	low-enriched U-10Mo
mA	milliampere(s)
mm	millimeter(s)
mol%	
PNNL	Pacific Northwest National Laboratory
SEM	scanning electron microscopy
μm	micron(s)
U-10Mo	uranium-10 percent molybdenum alloy
USHPRR	U.S. High Performance Research Reactor
V	volt(s)

Contents

Figures

Tables

1.0 Introduction

The mission of the U.S. High Performance Research Reactor (USHPRR) Conversion Program is to reduce and protect vulnerable nuclear and radiological material located at civilian sites worldwide. Fuel Development, Fuel Fabrication Capability (FFC), and Reactor Conversion are three principal program activities related to the conversion from highly enriched fuel to low-enriched uranium of six USHPRRs. Funded through the National Nuclear Security Administration NA-23 (Office of Material Management and Minimization), the FFC is establishing a manufacturing process for implementation by commercial entities to provide low-enriched uranium fuel after conversion from the USHPRRs' existing highly enriched uranium (HEU).

1.1 Purpose and Scope

The FFC commissioned Pacific Northwest National Laboratory (PNNL) to investigate manufacturing processes for the uranium-10 percent molybdenum (U-10Mo) alloy monolithic fuel. The low-enriched U-10Mo (LEU) has been identified as the most promising alternative to the current HEU used in the nation's fleet of USHPRRs. The nominal composition of the new monolithic LEU plate-type fuel in inches, shown in Figure 1.1, is U-10Mo fuel foil enriched to slightly less than 20 percent [235]U, a thin zirconium interlayer/diffusion barrier, and a relatively thick outer cladding of 6061 aluminum. The USHPRR Conversion Program is investigating several alternative approaches to rapidly determine the most cost-effective and robust method for manufacturing the plate fuel.
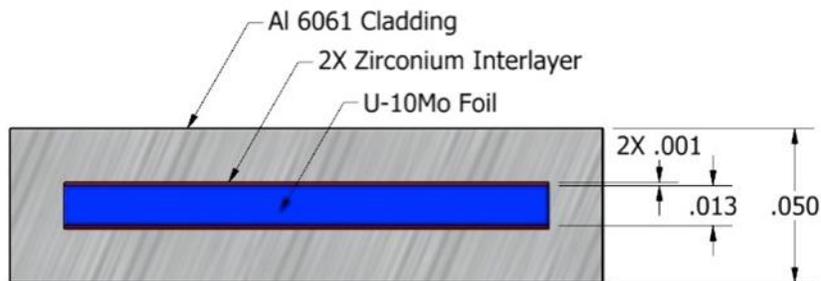
Figure 1.1. Nominal As-Bonded Geometry of the USHPRR U-10Mo Fuel Prior to Final Shaping

These alternative technologies have included electromagnetic pulsed joining, co-extrusion, chemical vapor deposition, and physical vapor deposition. The alternative technologies have been, or are being, investigated for applying the zirconium interlayer. The objective of the research documented herein was to develop a plating process that will produce a uniform zirconium metal coating nominally 25 μm in thickness onto U-10Mo foils. This process needs to be both reproducible and scalable.

1.2 Report Contents and Organization

The ensuing sections of this report present background on zirconium electroplating, followed by descriptions of the experimental methods, plating results, and related discussion and conclusions.

2.0   Background on Zirconium Electroplating

Electroplating (plating) has been used for many years as a very economical method for applying metallic coatings on metallic substrates. Typically, plating is associated with metals, such as chromium, nickel, and copper, which are deposited on steel from aqueous baths. The coating is accomplished by having ions of the metal in the conductive plating solution (electrolyte) that are "driven" to the substrate by an electrical potential. However, ions of many metals, such as zirconium, molybdenum, niobium, titanium, and uranium, cannot be held in an aqueous electrolyte without oxidizing, so traditional aqueous plating processes will not work. Therefore, plating of zirconium ions requires a different electrolyte, one that can retain a stable zirconium ion in solution. For metals such as zirconium, molybdenum, titanium, and uranium the electrolyte can be a molten salt. In a molten salt electrolyte, the zirconium is retained in an ionic form without oxidizing, which enables plating to occur in a manner similar to conventional aqueous solution plating.

Among the differences between salt and aqueous electrolytes are temperature, diffusion rates of the ions, and sensitivity to the surrounding environment. High temperatures are needed to keep the salt in a liquid form, and often combinations of salts are used to control the melting point. The diffusion rate of ions in the salt is slower. Sometimes, depletion of the ions near the cathode can occur, and in some cases it can alter the plating bath chemistry, local to the substrate, enough to stop the ion transport process. To avoid depletion, fully reversed pulsed electrical potentials can be used to allow the ions to diffuse thermally while no plating is occurring. The salts are sensitive to moisture absorption, which can cause oxidation of the ions and prevent plating; therefore, molten salt baths must be maintained in dry atmospheres, and plating must be performed under inert gas coverage. One advantage of molten salt plating is that, when the proper salts are used, the potential can be reversed, and even a substrate with a highly stable oxide, like uranium, can be cleaned by electrochemical reduction. Molten salt electrolytes that have been investigated include pure fluorides (Mellors and Senderoff 1965; Mellors and Senderoff 1966; Senderoff and Mellors 1966; Groult et al. 2011; Groult et al. 2008; Nissen and Stromatt 1968), pure chlorides (Basile et al. 1981; Flengas et al. 1968; Girginov et al. 1995; Kipouros and Flengas 1985; Lister and Flengas 1965; Malyshev et al. 2010), and mixed chlorides and fluorides (Malyshev et al. 2010; Guang-Sen et al. 1990).

Fluoride electrolytes have advantages with respect to the simplicity of reduction reactions (Mellors and Senderoff 1966; Malyshev et al. 2010). In these fluoride salt bath studies, the cathodic process was attributed to the reaction given in Equation (2.1) that involves a single step involving a four-electron transfer (Mellors and Senderoff 1966; Mellors and Senderoff 1965; Senderoff and Mellors 1966).

$$ZrF_6^{2-} + 4\ e^- \rightarrow Zr + 6\ F^- \tag{2.1}$$
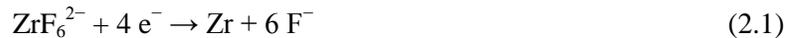
In a later study, Nissen and Stromatt (1968) used molten fluoride electrolytes to deposit zirconium metal onto uranium substrates. The conditions used in this study included a KF-LiF eutectic electrolyte containing 2 to 10 wt% ZrF_4, a Zr metal anode, a 635°C–675°C deposition temperature, and 20 to 40 mA/cm^2 current density. Nissen and Stromatt (1968) obtained coating thicknesses up to ~125 μm, while maintaining fine grain sizes and few pores. The bath required continuous purification, primarily to avoid moisture, to maintain coating quality. Other studies excluded KF from the molten salt electrolyte because of the possible reduction of potassium ions, as shown in Equation (2.2) (Mellors and Senderoff 1966).

$$Zr + nKF \rightarrow ZrF_n + nK \tag{2.2}$$

In more recent studies using a LiF-NaF-ZrF$_4$ eutectic electrolyte on carbon substrates, Groult et al. (2008, 2011) obtained very coarse dendritic deposits, as shown in Figure 2.1. (from Groult 2011).
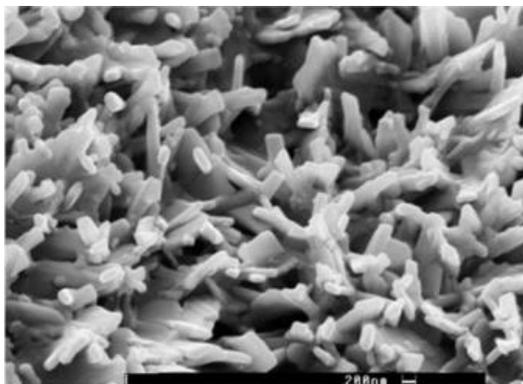
Figure 2.1. Resulting Zirconium Plating Structure, 650°C, LiF:NaF:ZrF$_4$ (26:37:37)

Reactions in chloride electrolytes have been found to be more complex than in molten fluorides; oxidation states 0, +1, +2, and +4 have been observed (Sakamura 2004). Multiple reaction steps have been reported, depending on the identity of the molten chloride constituents (Basile et al. 1981). Zr(IV) complexes were found to increase in stability following Li < Na < K < Cs (Flengas et al. 1968). Disproportionation reactions have been found to occur to a much larger extent than in fluoride electrolytes, as shown in Equation (2.3) (Basile et al. 1981).

$$2\,ZrCl_2 \leftrightarrow ZrCl_4 + Zr \tag{2.3}$$

Such reactions were found to be particularly accelerated if the electrolyte contained CsCl (Basile et al. 1981; Flengas et al. 1968).

In mixed chloride-fluoride salts, two-step reduction mechanisms are most widely reported. For example, Guang-Sen et al. (1990) described electrodeposition processes in NaCl-KCl-K$_2$ZrF$_6$, as shown in Equations (2.4) and (2.5).

$$ZrCl_{6-x}F_x^{2-} + 2e^- \rightarrow ZrCl_{6-x}F_x^{4-} \tag{2.4}$$

$$ZrCl_{6-x}F_x^{4-} + 2e^- \rightarrow Zr + (6-x)Cl^- + xF^- \tag{2.5}$$
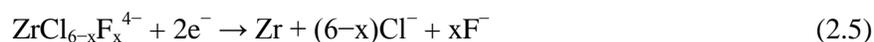
Disproportionation reactions, such as that shown in Equation (2.3), are also believed to occur.

Because of the reported advantages of the simplicity of electrodeposition due to the lack of disproportionation reactions, salt volatility, and corrosion, a eutectic mixture of LiF-NaF-ZrF$_4$ (26-37-37 mole %) with a eutectic temperature of ~450°C, was initially chosen, and was identical to that used by Groult et al. (2008, 2011). Other fluoride salts, such as KF and CsF, were not initially considered because of the potential potassium metal formation reported by Mellors and Senderoff (1966) and the possible oxidation reported by Nissen and Stromatt (1968). An additional sacrificial zirconium anode was used to minimize depletion of ZrF$_4$ over multiple plating experiments.

The major processing steps for the fabrication of plate using an electroplated Zr diffusion barrier are as follows:

1. Roll U-10Mo foil to final thickness.

2. Shear it to final fuel dimensions.

3. Clean and dry the fuel foil.

4. Load the fuel into the plating system.

5. Polarize the U-10Mo foil.

6. Insert the U-10Mo foil into the salt bath (electroplate).

7. Switch to pulse plating to build depth.

8. Remove the plated foil from bath.

9. Wash dried salt off the plated foil and dry it.

10. Hot isostatic press the fuel in an aluminum can.

2.1   Zirconium Metal Thickness/Current Density Relationship

When the ZrF_4 melts, it introduces Zr^{4+} ions into the molten salt, though not necessarily in that form. Complex ions, such as $Li_2ZrF_6^{2-}$ and $Na_2ZrF_6^{2-}$, are also possible, as well as ZrF_x^{4-x}, where x = 4 to 8E-17. With the introduction of electrons, the zirconium ions are reduced to zirconium metal via the overall reaction of Equation (2.6). The plating thickness, x_{Zr}, in micrometers, is given as Equation (2.7).

$$Zr^{4+} + 4e^{1-} \rightarrow Zr^0 \qquad (2.6)$$

$$x_{Zr} \, (\mu m) = It \, FW_{Zr}/4x10^4F\rho A \qquad (2.7)$$

where
$\quad I \;=\;$ the current density (A/cm^2)
$\quad t \;=\;$ time in seconds
$\quad FW_{Zr} \;=\;$ is the formula weight of zirconium
$\quad F \;=\;$ the Faraday constant,
$\quad \rho \;=\;$ is the density of Zr
$\quad A \;=\;$ the surface area to be plated.

It is important to note that this is an idealized situation that holds true only if all of the current is consumed in the reduction of the zirconium onto the metal substrate. Typical plating achieved from the LiF-NaF-ZrF_4 bath is in the 10 percent range. For the zirconium metal system, these inefficiencies may at least partially result from side reactions involving the partial reduction of Zr^{4+} to Zr^{2+} at the cathode, and re-oxidation of Zr^{2+} at the anode. In this way, current would be consumed without actually plating out on the U-10Mo foils.

3.0   Experimental Methods

Experimental methods and the apparatus are described below.

3.1   Plating Bath Compositions for Zirconium Plating onto U-10Mo

Five different compositions of the plating bath were evaluated during this effort:

1. LiF:NaF:ZrF$_4$ = 26:37:37 mol%

2. LiF:NaF:KF = 46.5:11.5:42 mol%

3. LiF:NaF = 61:39 mol%

4. LiF:NaF:ZrF$_4$ = 60.75:38.75:0.5 mol%

5. LiF:NaF:ZrF$_4$ = 60.5:38.5:1 mol%.

The molten salt plating bath constituents were LiF (purity 99.995%), NaF (purity 99.99%), KF (purity 99.99%), and ZrF$_4$ (purity 99.99%); they were procured from Sigma–Aldrich. The separate chemicals were weighed and compounded within a glove box because of their moisture sensitivity, and placed into the plating crucible. The crucible was wrapped in Parafilm during the transfer from the glove box to the plating apparatus. Next, the salt was dried in the plating apparatus using a purge of dry, O$_2$-free argon, which was passed through a getter. This purge was continued until the volume equivalent of seven complete gas exchanges had occurred; the purge flow was decreased and the salt was heated at a ramp rate of 1°C per minute to a maximum temperature of 250°C for 8 hours. At this point, the salt bath was heated to 850°C, which is above the melting point of the LiF, and held at that temperature for 1 hour. With the liquid LiF present, the other two constituents dissolved into the solution, creating the eutectic mixtures.

3.2   U-10Mo Substrate/Cathode Preparation

For the entire scope of this effort, 635 µm thick U-10Mo foils were used as the cathode in the plating trials. The foils were produced from a coupon produced at the Y12 National Security Complex, in Oak Ridge, Tennessee, and labeled 3rd Andrew (A3). To produce the coupon, a plate was cast approximately 12.7 cm × 17.8 cm × 0.5 cm and surface machined to a 3.76 mm thickness. The plate was then sectioned into 1.9 cm × 2.3 cm rolling samples at Energy Solutions – MSC, Oak Ridge, Tennessee. Some samples were then homogenized at 900°C for 48 hours in an inert atmosphere furnace and hot rolled at 650°C with a 15 percent reduction per pass, to a final thickness of 635 µm. Other samples were hot rolled without homogenization. The 635 µm foils were then sheared to 3.2 mm × 3.8 cm long strips for cathodes. The plating foils/cathodes were etched in 8 molar nitric acid for 10 minutes (obvious reaction stopped in 3 minutes), rinsed with deionized water, and dried by rinsing in ethanol. Plating occurred within 1 hour of the final ethanol rinse.

3.3   Molten Salt Plating Apparatus

The initial apparatus was modeled after high-vacuum systems and glove boxes. It has an externally heated high-temperature capability, low pO$_2$/pH$_2$O chamber with a large gate valve to an antechamber,

into which the cathode can be loaded while maintaining a seal between the low pO_2/pH_2O chamber to avoid exposure of the molten salt bath to the atmosphere. This apparatus was assembled from valves and electrical and thermocouple feed-throughs suitable for high-vacuum and inert gas atmospheres. The initial material used for the high-temperature, low pO_2/pH_2O chamber was an alumina cover tube; it was later changed to an Inconel[1] 600 pipe. Standard pipe flanges were used to connect the gate valve and cover tube. The gate valve and the antechamber were made of 316 stainless steel. Teflon[2] gaskets were used on the pipe flanges, and a fluorinated ethylene propylene O-ring was used on the seal to the alumina tube. Where possible, such as on the Inconel tube, the flanges were welded. Packing on the gate valve had to be changed out to Teflon packing, because the original packing became a source of carbon contamination. A schematic of the final apparatus with the Inconel tube and a photograph of the initial system are shown in Figure 3.1.
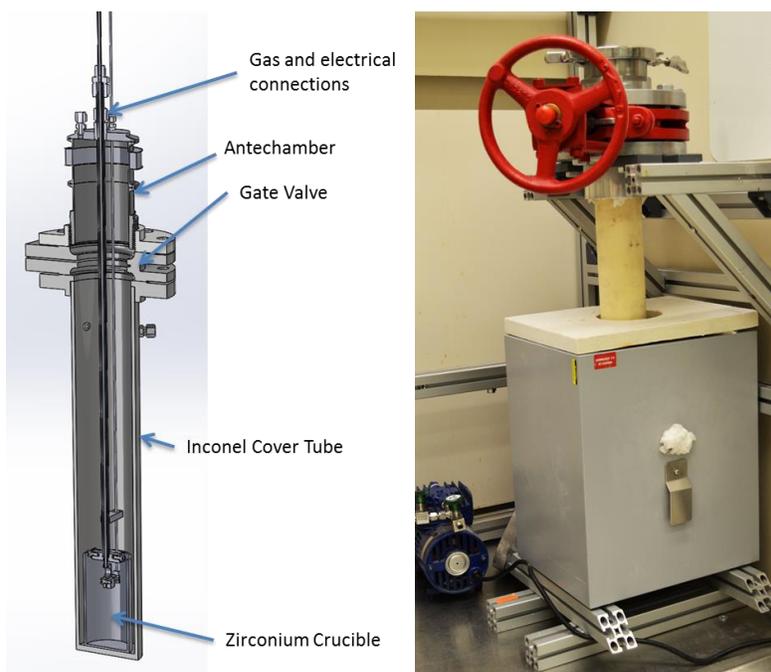
Figure 3.1. Schematic and Photograph of the Experimental Apparatus

3.4   Electrode Configurations and Plating Head Used

The U-10Mo foil cathode dimensions were 0.32 cm × 3.81 cm × 0.64 mm and gripped so that 1.91 cm could be submerged into the molten salt. Two different cathode holders were used. The first configuration used a plating head constructed of alumina. This alumina holder initially held a single molybdenum substrate cathode that was spot welded to the platinum connection wires, as were the zirconium foil anodes (250 μm thick) on either side. The anode dimensions were 1.91 cm × 5.08 cm. In later experiments, the anode configuration was changed to a single sheet that was bent into a u-shape to improve the zirconium plating uniformity around the end of the cathode. This cathode holder also held the zirconium foil reference. A schematic of the initial cathode/sample holder is shown in Figure 3.2. The plating head design was changed to accommodate the higher currents required to prevent UF_x

---

[1] Inconel is a trademark of the Special Metals Corporation group of companies.
[2] Teflon is a trademark of the E.I. du Pont de Nemours and Company.

formation and to be able to plate the larger approximately 2.5 cm x 12 cm Mini-Plate-1 (MP-1) test samples. The current leads were two coaxial Inconel tubes electrically isolated with an alumina insulator on the higher temperature end and a polymer fitting on the cold end. To change out the samples quicker, both the anode and cathode contact were redesigned to use clamps, eliminating the welding step. Two platinum leads in alumina thermocouple tubing were run down the center of the current tubes and used to measure the plating potential at the sample. A schematic of the second sample holder is shown in Figure 3.3. The sample clamp was made of nickel. The pO_2 in the chamber was low enough to keep the nickel from oxidizing, providing a consistent electrical contact, but some interaction between the nickel metal and the uranium was observed. Molybdenum may have been a better choice for the clamp material. No interaction between the nickel and the zirconium anode was observed during testing.
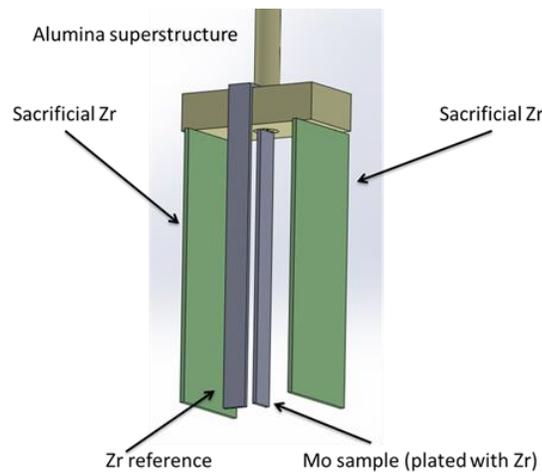
Figure 3.2. Initial Sample Holder
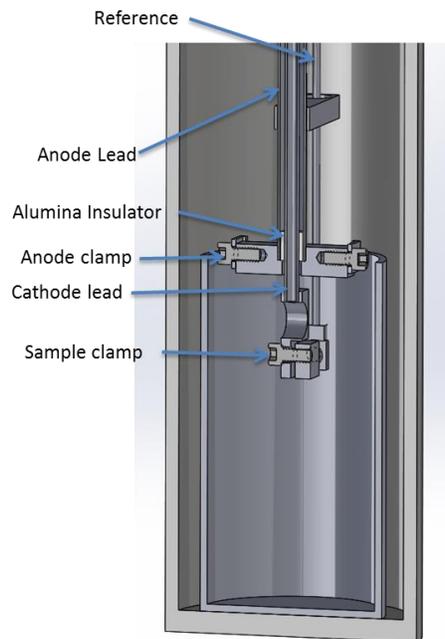
Figure 3.3. Second Sample Holder Configuration

3.3

3.5 Testing Procedure

The foils were either welded or clamped onto/into the sample probe assembly. This probe assembly was then installed on the plating apparatus with the sample inside the antechamber section of the apparatus. The upper chamber was purged for more than seven complete atmosphere exchanges (typically 10 minutes at 200 SCCM). The large gate valve was opened and the sample was lowered into the furnace hot zone, but not into the molten salt electrolyte. At this point, the electrical connections were established. For the insertion polarization experiments, the insertion potential was initialized and the sample was lowered into the molten salt bath. As the sample touched the surface of the electrolyte, current began to flow, and the sample was lowered an additional 2.5 cm. As this same electrical continuity was established, zirconium was plated onto the sample. With the non-insertion potential samples, the open cell potential was monitored during the final lowering of the sample. Once the sample touched the surface of the electrolyte, the open cell potential stabilized, and the sample was then lowered 2.5 cm farther into the melt. The direct or pulsed plating was then initiated. Upon completion of the plating electrical cycle, the sample was slowly raised into the antechamber to minimize heating of the sliding seals in the probe assembly. The large gate valve was then closed, the probe assembly was removed, and the sample was removed.

4.0   Plating Results

A set of test conditions that produced a good zirconium plate onto molybdenum was developed during the previous development effort (Coffey et al. 2014). Unfortunately, when this same procedure was attempted on U-10Mo, UF_3, and possibly some UF_4 (here after referred to as UF_x), was produced on the foil. This was caused by the spontaneous reaction between ZrF_4 and uranium metal to form UF_x. This reaction occurred at all temperatures when the bath was molten, and at all concentrations of ZrF_4. The literature did not mention this reaction, and the focus of this year's research was on plating and alternative bath chemistries that would exhibit a lower propensity to form the UF_x. Two main concepts were pursued to prevent UF_x from forming: 1) increase the cathodic potential on the U-10Mo above the free energy of formation for the UF_x, thereby preventing the UF_x from forming on the foil, and 2) use alternative bath chemistries consisting of either mixtures not containing ZrF_4, which would therefore not react with the uranium, or mixtures containing a lower concentration of ZrF_4 to lower the reaction rate and make it easier to prevent the reaction with cathodic potential.

4.1   LiF:NaF:ZrF4 Bath and Insertion Potential Experiments

The formation of UF_x and the voltage insertion experiments are discussed in this section.

4.1.1   Formation of Uranium Fluoride

The LiF:NaF:ZrF$_4$ mixed salt bath at a mixture of 26:37:37 mol%, respectively, was used to produce good plating on molybdenum surrogate samples. When this bath and the plating parameters were attempted on U-10Mo samples, significant amounts of UF_x were formed. One such sample is illustrated in Figure 4.1. The zirconium metal on this sample may not have all come from electroplating; it may have also come from the complete reduction of the ZrF_4 to Zr metal by the uranium. Three reactions between the ZrF_4 and the uranium metal are energetically favorable to form:

1) $U + 3ZrF_4 = 3ZrF_3 + UF_3$

2) $U + ZrF_4 = Zr + UF_4$

3) $U + 1.5\ ZrF_4 = 1.5ZrF_2 + UF_3$.
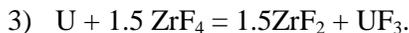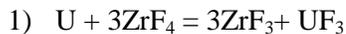
The plots in Figure 4.2 show the formation energies of these reactions as a function of temperature and the corresponding cathodic potential needed to prevent their formation. ZrF_3 may not form because of the low activation energy, but there is evidence that the zirconium metal is forming in the absence of plating voltage. Figure 4.3 shows the results of the U-10Mo sample inserted into the salt bath with no applied potential and then allowed to react for 10 minutes. There is clearly a thin layer of zirconium metal on the outside of the UF_x layer. This occurrence is only possible if the uranium metal reduces the ZrF_4 completely.
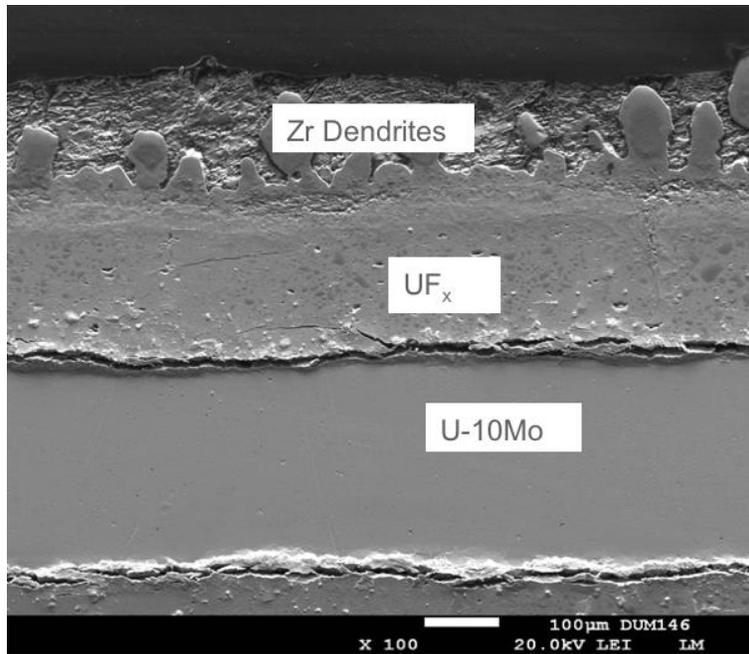
Figure 4.1. Fully Homgenized Depleted U-10Mo Plated with Zirconium Metal Zero Insertion Potential, Exhibiting Extensive UF_x Formation and Dendritic Growth
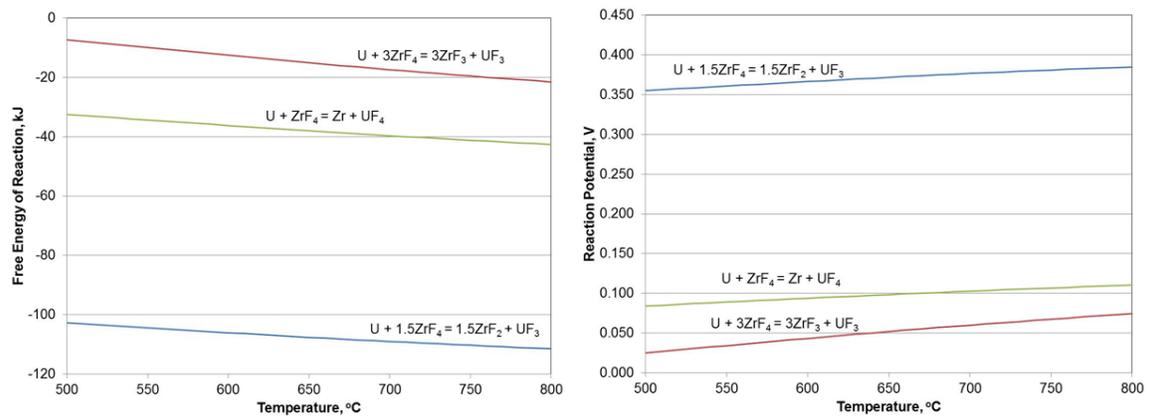
Figure 4.2. Calculated Free Energy of Formation and Required Cathodic Potential to Prevent Interaction of ZrF_4 and Uranium
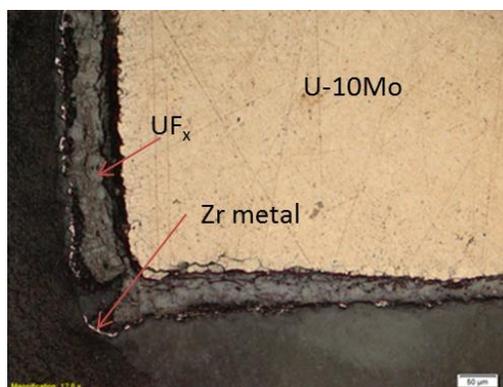
Figure 4.3. U-10Mo Sample Inserted in Salt Bath, with No Potential for 10 Minutes

4.1.2   Voltage Insertion Experiments

In an attempt to prevent the uranium from reacting with the ZrF_4, a number of tests were conducted where the U-10Mo was inserted into the bath with an applied potential above that needed to prevent the UF_x from forming. The insertion voltage was varied between 0.275 V and 5 V in an effort to mitigate this problem. The voltages were measured as a 4-point measurement taken at the sample and anode just above the salt surface. The measurements include the anode and cathode polarizations, the bath resistance, and some of the ohmic loss from the current flow in the sample and anode. At potentials of less than 1 V, the uranium was not protected from forming UF_x. At a 1 V insertion potential, most of the sample was protected, but the edges still had moderate dendritic growth and some UF_x formation. The sample shown in Figure 4.4a and b shows a cross section perpendicular to the longest dimension of the sample and parallel to the surface of the salt. The cross section is approximately in the middle of the section that was submerged in the salt, as shown in Figure 4.5. In Figure 4.4a, it is observed that the adherent plating starts at 40 μm from the end, but a UF_x coating is underneath the plating from the end to about 40 μm from the end. Figure 4.4b is a higher magnification of the upper left-hand corner of Figure 4.4a, where UF_x and zirconium dendrites formed on the edges. The edges of the sample are perpendicular to the anode electrode. Therefore, because of the longer field lines, these edges may not have seen as high a potential as the two faces of the sample that are parallel to the anode. In addition, it appears that wherever UF_x is present, zirconium dendrites will usually be growing over the top of it. This may be the result of zirconium metal seeds formed initially by the reaction of the ZrF_4 and uranium that in turn grew into dendrites.
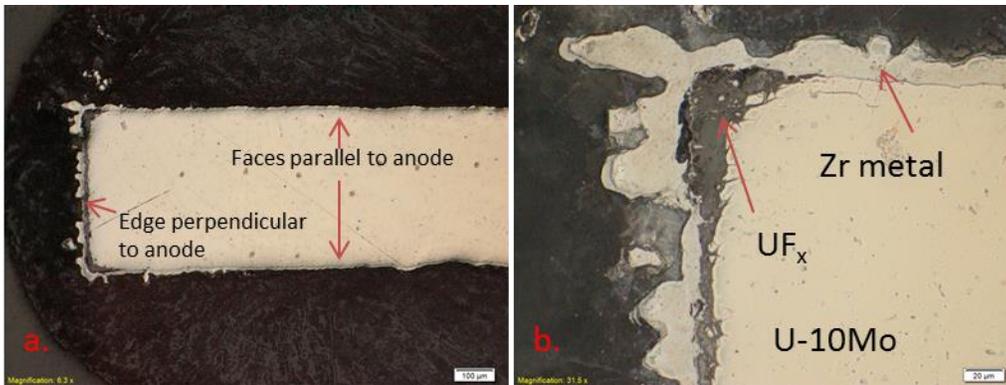
Figure 4.4. U-10Mo Sample with 1V Insertion Potential, Incomplete Encapsulation of Edge, and Resulting Dendritic Growth. Figure 3.4b is a higher magnification of the upper left-hand corner of Figure4.4a.
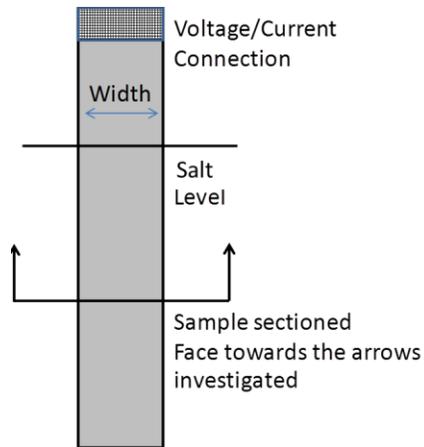
Figure 4.5. Schematic of Sample Cross Section Used for Analysis

Increasing the insertion voltage to 2 V resulted in a sample with complete encapsulation and a thickness of 15 μm ± 5μm. Dendritic growth was present across the sample. Figure 4.6 shows both edges of the 2 V sample that was cross-sectioned the same as the 1 V sample, at 100X magnification. No UF$_x$ was found on the sample. The U-10Mo sample had complete wrap-around coverage at the ends perpendicular to the anode, but the dendritic growth was higher than desired.
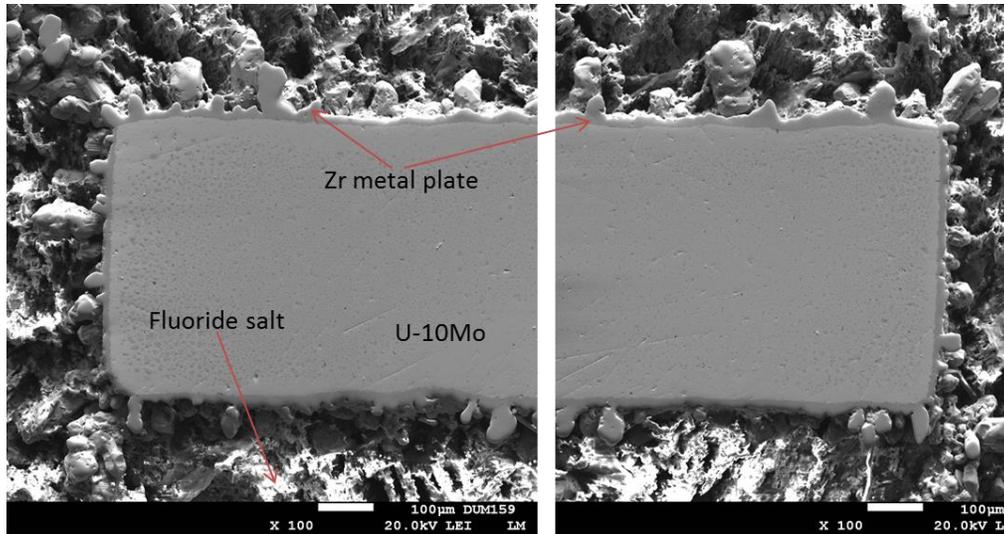
Figure 4.6. Scanning Electron Microscope Image of the 2-V, U-10Mo Sample, at 100X Magnification, No UFx is Found Between the Zr and the U-10Mo, and the Zr plating completely encapsulates the U-10Mo.

The U-10Mo samples used for the 1 V and 2 V tests were homogenized prior to hot rolling; this yielded a complete encapsulation by the plated zirconium metal. However, when reproducing the 2 V test with a sample of the U-10Mo rolled without homogenization, the results were vastly different. The 2 V charge was no longer sufficient to prevent the UF_x formation, as shown in Figure 4.7, where the sample was plated under the same conditions as the sample in Figure 4.8. More tests were conducted with an unhomogenized batch of U-10Mo material at higher voltages to see if the UF_x formation could be suppressed. Even at voltages as high as 5 V, UF_x formed. Higher voltages could not be used, because the ZrF_4 started to break down at cathodic potentials greater than 4 V. The reason the plating was so sensitive to sample heat treatment was not understood. It was impossible to plate zirconium on a U-10Mo sample that was not homogenized due to the formation of the UF_x layer. After these tests all future plating trials were performed on rolled samples derived from homogenized castings.
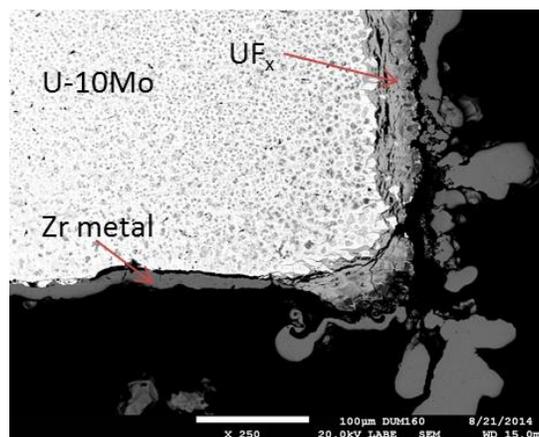
Figure 4.7. Sample of the rolled U-10Mo without Homogenization Plated at 2 V. Some regions have no UF_x while others show significant amounts.

4.2 LiF:NaF Fluoride Bath

The initial salt bath composition looked promising at elevated voltages on small samples. However, these same conditions would have been difficult to scale up. Maintaining a sufficient voltage over the length of a 122 cm (4 ft) long sample would have been challenging because of the ohmic loss associated with the U-10Mo resistance. This would be especially true because these voltages correspond to high current densities (>2 amp/cm^2). Therefore, the approach was to try a salt bath that did not contain any ZrF$_4$. Two salt bath compositions were selected: the LiF:NaF eutectic and the KF:LiF:NaF eutectic.

The ratio of LiF to NaF in the LiF:NaF plating bath was 61 to 39 mol%. This salt bath did not contain any ZrF$_4$, and therefore did not react with uranium to form UF$_x$. The eutectic temperature of this bath was 652°C, which is much higher than the 436°C of the initial bath mixture NaF:LiF:ZrF$_4$. Realistically, the lower temperature limit on plating with the bath was around 700°C. The initial goal of this work was to determine if ZrF$_4$ was necessary in the salt mixture to electroplate, and to find the experimental parameters that would allow good zirconium plating to occur. Both direct current (DC) and pulsed plating experiments were used in these preliminary scoping studies, but DC was investigated first. The nominal cell resistance was near 1 ohm. With no ZrF$_4$ in the bath to react, some of the samples were reverse-polarized at the initiation of the test to clean the surface of U-10Mo. This did not seem to improve the plating, and may have been detrimental because of the roughening of the sample surface occurred. The sample shown in Figure 4.8 was run with a reverse polarization of 0.125 amp for 5 seconds, and then DC-plated for 10 minutes at 0.5 amp at ~0.46 V. Only a very small amount of zirconium was seen on the surface of the sample. The DC experimental matrix is given in Table 4.1.
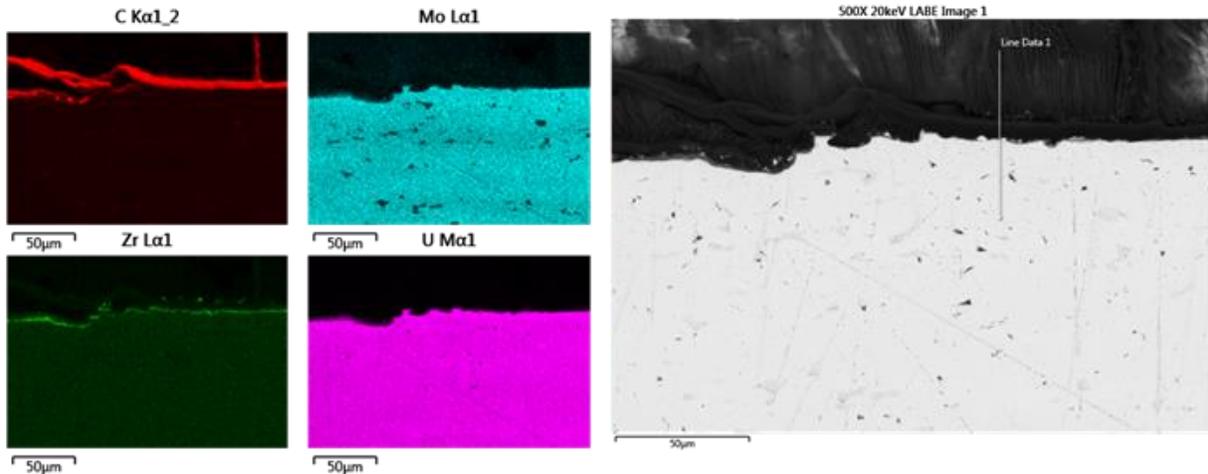
Figure 4.8. DC Plating 10 Minutes at 0.5A at ~0.46 V with an Initial Reverse Polarization Pulse

Table 4.1. LiF:NaF DC Plating Experimental Matrix

Temperature, °C	754	755	755	756	790	798	800
DC Current, A	0.05	0.75	1.75	0.50	0.50	1.30	1.50
DC Potential, V	0.05	0.69	1.61	0.46	0.46	1.20	1.38

Although only a small amount of plating was found on the sample cross section, a significant amount of plating was observed. However, the majority of plating was in a thin sheet just at the surface of the melt. The cause of this is currently unknown. It was as if the majority of the current passed in a narrow band near the top of the salt bath. On these samples, what appeared to be a thin foil of zirconium metal formed at the top of the uranium sample and radiated out toward the anode. The foil then folded down over the sample as it was pulled from the bath, because it no longer had the support of the molten salt. This was noticed to some extent with other baths, but was much more noticeable with this one. The higher operating temperature may have been a contributing factor. There also may have been a contaminant in the bath that caused the salt surface to be more conductive. An interesting test would be to increase the distance between the anode and cathode to see if it changed this effect. However, with the existing setup, this was not feasible. Running the DC plating at a higher current produced more—but not significantly more—plate on the sample surface. However, more material was deposited at the top of the sample, as shown in Figure 4.9.
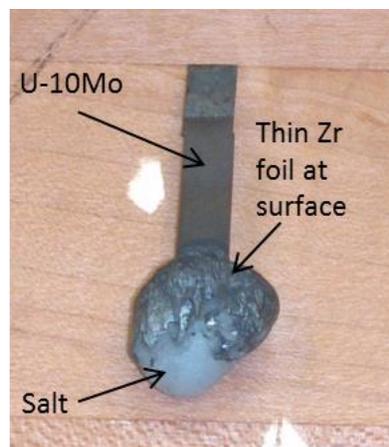
Figure 4.9. Sample was DC-Plated at 1.3A for 30 Minutes, Showing Extensive Growth of the Foil Extending from the Top of the Sample

Pulse plating at lower currents decreased the amount of material deposited at the top of the sample and produced thicker plate on the lower sections of the sample. The sample shown in Figure 4.10 was pulse plated at 0.25A for 2.5 seconds with a 9-second rest before reapplying the pulse. This was repeated for 325 cycles, and took approximately 1.5 hours. The total time is longer than one would calculate, because there are a few seconds in the switching delay of the instrument. The plating thickness was close to what was desired; however, at the temperature the plating was occurring, the zirconium started to react with the molybdenum in the U-10Mo alloy, as shown in Figure 4.11. In some places, more than half of the plating reacted with the molybdenum (likely forming Mo_2Zr). The pulse plating experimental matrix is given in Table 4.2. There was still significant dendritic growth; this may have decreased with the correct parameter set. However, with the long times needed at the high temperature, it was highly probable that any zirconium plate produced would be largely reacted with the molybdenum; thus, the decision was made to abandon this salt bath composition.
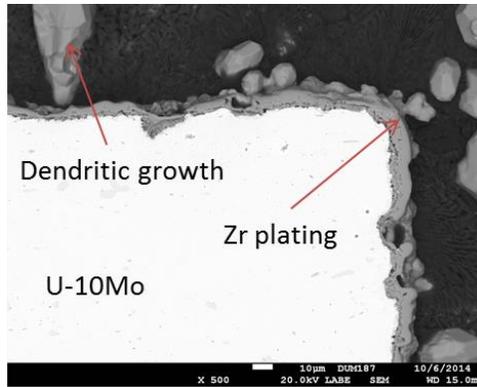
Figure 4.10. LiF:NaF Pulsed Plating Sample
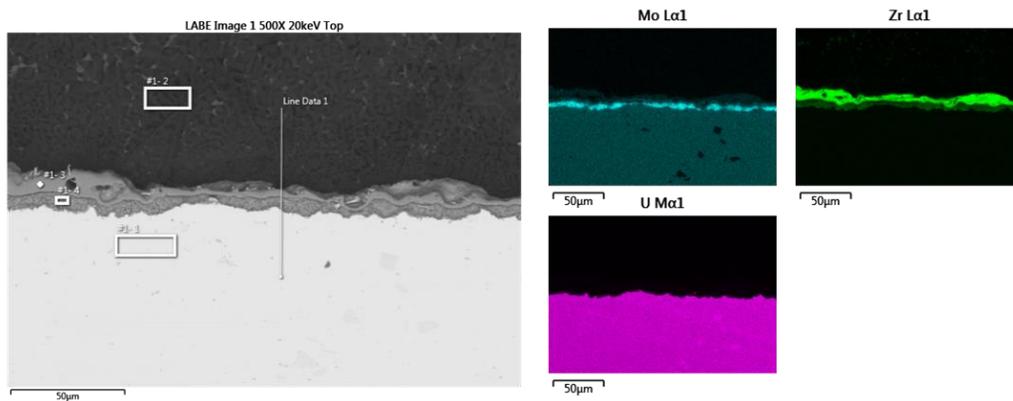
Figure 4.11. LiF:NaF Pulsed Plating Sample with Interaction Between the Mo and Zr

Table 4.2. LiF:NaF Pulsed Plating Experimental Matrix

Temperature, °C	Current, A	On Time, Sec	Off Time, Sec	Cycles
747	0.5	5	5	120
759	0.5	2.5	5	240
749	0.5	2.5	5	240
782	0.25	2.5	9	325
782	1	2.5	3	120

4.3 LiF:NaF:KF Bath

After showing ZrF_4 was not necessary for plating, it was speculated that if a lower temperature salt mixture was used, it might be possible to find pulse-plating parameters to decrease the dendritic growth and minimize the amount of interaction between the molybdenum and zirconium. The eutectic ratio of LiF:NaF:KF in this plating bath was 46.5:11.5:42 mol%, respectively. The eutectic melting point was 454°C, with a realistic lower plating temperature of around 500°C. This is quite similar to the temperature range for the original LiF:NaF:ZrF_4 bath.

4.8

The KF:LiF:NaF composition behaved differently than the other bath compositions. In the literature, there are reports of the KF being reduced by zirconium to form potassium. This reaction has a positive delta G of formation, and therefore, should not happen. In addition, this is the same system used by the original Nissen and Stromatt (1968) paper. However, some samples began to smoke upon removal from the bath, once they were exposed to the humidity in the room air. This is an indication that potassium was somehow forming. This seemed to happen when the voltages were higher, but they were still far below the breakdown voltage of KF, which is above 5 V. A sample that appeared to have formed potassium is shown in Figure 4.12. The areas that began to smoke formed white tendrils on the surface of the sample. It is possible another reaction was occurring, or one that was being activated at voltages lower than the breakdown voltage. The nature of this reaction was never elucidated.
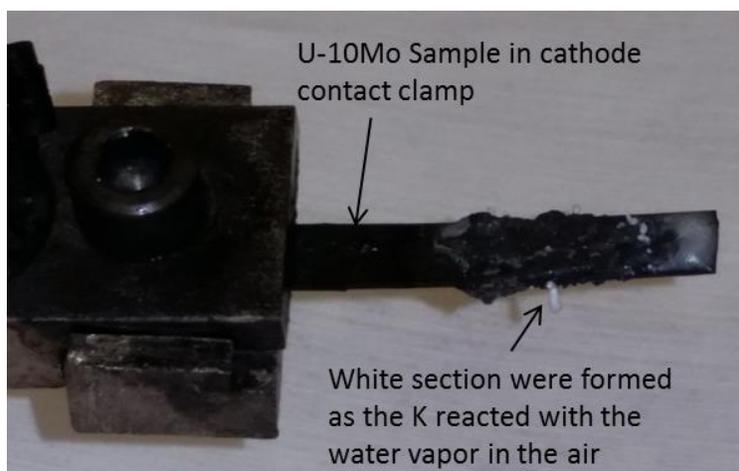
Figure 4.12. U-10Mo Sample Pulse Plated 0.5A for 2.5 Seconds, 3 Second Rest, 120 Cycles

Another issue with the KF-containing bath was the hydroscopic nature of the KF. With the previous bath compositions, the sample was removed and mounted in epoxy to be cross-sectioned for optical microscopy and scanning electron microscopy (SEM) with the salt still on it. When this was attempted with the KF-containing salt, the KF started hydrating by pulling water from the humidity in the room. This in turn started forming HF, as some of the KF reacted with the water, and the HF started to dissolve the sample. However, this was also one advantage of the KF system, because KF is highly soluble in water, making salt removal quick and easy. The salt was completely removed after only a few minutes in an ultrasonic water bath. This same method for removing salt had almost no observable effect on the bath compositions that did not contain KF. These KF-free salts required either mechanical removal of the salt or boiling water to dissolve the salt in a reasonable amount of time. The standard procedure for samples plated in the KF-containing bath was to remove the sample as quickly as possible from the plating head, place it in a Nalgene container of deionized water, and then place the container in an ultrasonic bath for 1 minute. The sample was pulled from the water, dipped in ethanol, and allowed to dry. The sample was then mounted in epoxy and cross-sectioned for analysis.

The effect of temperature on plating was studied using both the DC and pulsed regimens. The respective experimental matrices are given in Table 4.3 for the DC study and Table 4.4 for the pulsed-plating temperature studies. The experimental matrix used to determine the effect of plating current during the pulsed-plating regimen is shown in Table 4.5. This plating bath does not contain any ZrF_4, and therefore does not allow the formation of any UF_x, so no potential was applied to the sample before

insertion into the salt bath. Upon removal from the bath and cleaning off the salt, the samples appeared to have a light gray coating, which was quite promising. However, only small amounts of zirconium metal were found on the surface, as shown in Figure 4.13. Some of the zirconium plate could have been removed along with the salt, but this would only have been an issue if the plating was not well adhered. In addition, no dendrites were observed on these parts. It is possible that this bath was less susceptible to forming dendrites, or that they were removed during the ultrasonic salt cleaning step.

Table 4.3. LiF:NaF:KF DC Plating Experimental Matrix

Temperature	DC Current	DC Potential
524	0.25	1.6
600	0.0625	0.4
600	0.125	0.8
620	0.0625	0.4
625	0.0625	0.4

Table 4.4. LiF:NaF:KF Pulse Plating as a Function of Temperature Experimental Matrix

Temperature (°C)	Cycles	Current, A	On Time, Sec.	Off Time, Sec.
504	120	0.125	2.5	3
512	120	0.125	4	10
520	120	0.125	4	10
536	360	0.125	4	10
536	360	0.1275	4	30
550	120	0.125	4	10

Table 4.5. NaF:KF Pulse Plating as a Function of Temperature Experimental Matrix

Temperature, C	Cycles	Current, A	On Time, Sec.	Off Time, Sec.
504	60	0.075	2.5	3
504	240	0.075	2.5	6
504	8	0.1	2.5	3
504	120	0.125	2.5	3
501	120	0.25	2.5	3
504	10	0.25	2.5	3
501	120	0.5	2.5	3
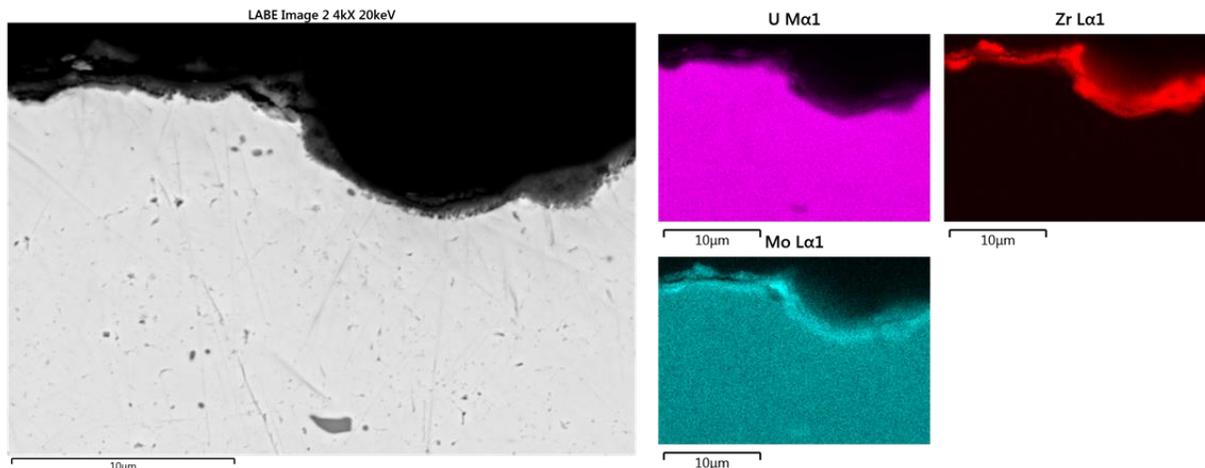
Figure 4.13. U-10Mo Samples Plated in the KF-Containing Bath 0.125A for 4 Seconds with a 10-Second Rest for 240 Cycles at 520°C

Another problem encountered with the KF-containing bath was that the KF vaporized and condensed on the plating head. This in turn started corroding the plating head after removal from the plating chamber and exposure to humidity in the air. This required one partial rebuild and one total rebuild of the plating head. Because of the inability to produce well-plated foils, and the highly corrosive nature of the KF:LiF:NaF bath, the decision was made to abandon this salt bath composition. The bath was changed to a LiF/NaF bath with a reduced amount of ZrF_4.

4.4   LiF:NaF + Low Concentration ZrF_4

It was proposed that the introduction of a small amount of the zirconium ion to the molten salt electrolyte would allow plating, but would also reduce the amount of UF_x that might occur. This small amount of the ZrF_4 did not move the melting point much, so the plating temperature was still 700°C or higher. The hope was that the addition of ZrF_4 would increase the rate at which the plating occurred and would minimize the time at temperature. If the time could be kept short, then the molybdenum and zirconium would have minimal interaction. In addition, this concentration of ZrF_4 was close to the concentration used in the original Nissen and Stromatt (1968) paper. Based on this line of thought, two ZrF_4 concentrations were investigated: 0.5 and 1.0 wt% were added to the eutectic mixture of LiF and NaF.

Only a few tests were conducted with the 0.5 wt% ZrF_4 concentration. During the time of this testing, the program had contacted Plasma Processes, a commercial vendor that does similar plating using molten salt electrolytes. This vendor used a very short reverse polarization on its parts to minimize dendritic growth. Due to the limitation of the PNNL test equipment, the shortest pulse achievable was a 1-second pulse. The sample shown in Figure 4.14 had a constant current of 0.2 amp applied to prevent UF_x from forming. On top of this constant DC current, a pulse of 1 amp for 2 seconds was applied, followed by a 20-second rest. This cycle was repeated for 10 cycles, and then 1 amp of reverse current was applied for 1 second. The entire sequence was repeated for 10 cycles. The sample showed some zirconium on the surface of the uranium, but the zirconium did not appear to be a coherent plate; it appeared to be particulate and an aggressive attack of the U-10Mo resulted in roughness. The SiO_2 contamination likely came from the polishing step, which used colloidal silica.

4.11

With no apparent UF$_x$ formation, the concentration of ZrF$_4$ was increased to 1 wt% after the first two tests. The conductivity of the bath was quite high. During DC cleaning runs, currents up to 4A would only have voltages of around 0.4 V. This corresponds to a resistance of 0.1 ohm, compared to the original 37 mol% ZrF$_4$ bath that had a resistance near 1 ohm. The concern was that cathodic potentials were too low to convert the Zr^{4+} all the way to zirconium metal, and that they were just being converted to Zr^{2+}. Therefore, the current density was increased in an attempt to obtain a higher voltage. Because of the limitation of the test equipment, the maximum current tested was 5 A during the pulse. Even this sample showed little apparent plating in the optical analysis. The experimental matrix for these experiments is shown in Table 4.6.
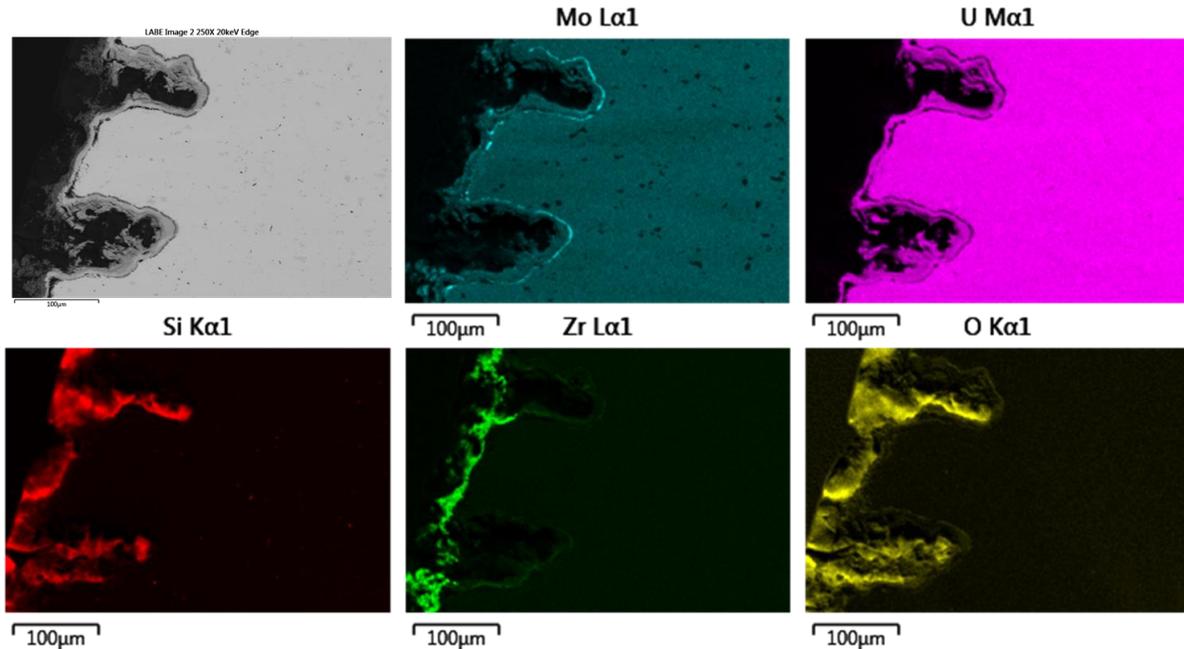
Figure 4.14. U-10Mo Samples Plating in 0.5 wt% ZrF4. The zirconium appears to be particulate and not a coherent plate.

Table 4.6. Test Matrix of LiF:NaF with ZrF$_4$ Addition. The first two rows had 0.5 wt% the rest were at 1 wt%.

Temperature, C	DC Current, A	Cycles	Pulsed, Current, A	Pulsed On Time, Sec.	Pulsed Off Time, Sec.	Reverse Current
750	0.2	100	1	2	20	1A, 1 sec. every 10th cycle
750	0.5	100	1.5	2	15	1A, 1 sec. every 10th cycle
750	0.5	100	1	3	20	1A, 1 sec. every 10th cycle
750	1.5	100	1.5	3	20	1A, 1 sec. every 10th cycle
712	2	25	3	3	20	4A, 1 sec. every 5th cycle

5.0 Discussion

The use of a molybdenum surrogate to establish a plating system, although beneficial, did not adequately represent U-10Mo because of the reaction of uranium with ZrF_4. Different testing conditions and salt bath mixtures were attempted during this effort with varying success. The most successful plating was achieved with the $NaF:LiF:ZrF_4$ bath using an applied potential during sample immersion.

A number of factors may have made the $NaF:LiF:ZrF_4$ bath perform the best. As the concentration of the ZrF_4 decreased in the salt bath, the conductivity of the bath increased. The conductivity of the $NaF:LiF$ bath with no ZrF_4 is almost 4 times that of one with 29 mol% ZrF_4 (Salannea et al. 2009) (Figure 5.1). This is an important factor, because it appears that the main driver for obtaining plating was when the ZrF_4 in the bath had sufficient cathodic potential. Looking at the plot on the cyclic voltammetry (Figure 5.2), the potential should be around 1 V to convert the Zr^{4+} directly to zirconium metal. On many samples the currents were exceptionally high (>1 amp/cm²), yet minimal to no plating was observed. One of the samples in the $NaF:LiF:ZrF_4$ bath had few dendrites, making it possible to reasonably estimate the plating efficiency. The value calculated was approximately 8 percent, raising the question of where the current was going. The most likely scenario was that if the voltage was not high enough the Zr^{4+} was most likely converted to Zr^{2+}, which in turn is converted back to Zr^{4+} at the anode. This results in an electrical circuit in the bath, but produces little or no plating. However, this only works for the bath compositions that contained ZrF_4.
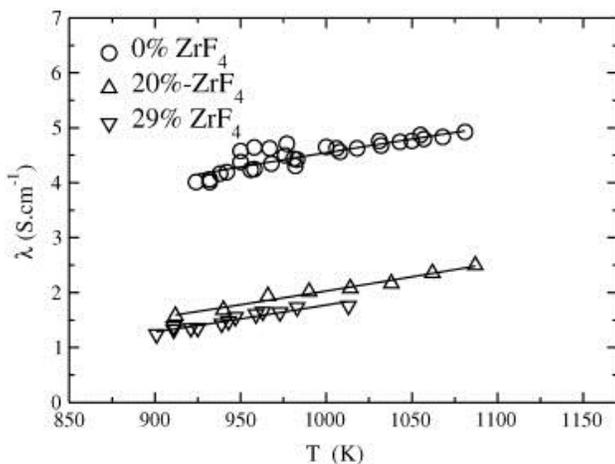
Figure 5.1. Electrical Conductivity of NaF:LiF Eutectic with ZrF_4 Additions
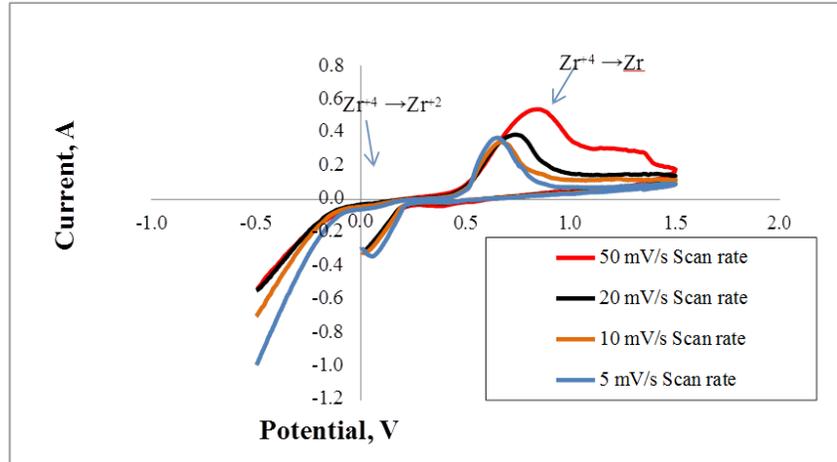
Figure 5.2. Cyclic Voltammetry (CV) Scan Showing Zr^{+4} Going to Zr Metal, and Zr^{+4} Going to Zr^{+2}

The bath compositions that did not have ZrF_4 behaved differently. When using the NaF:LiF bath, when high DC currents were used, the majority of the plating occurred near the surface of the melt, but when lower pulsed currents were used, reasonably good plates were achieved. The mechanism for this was never understood. Because of equipment limitations, the time scale of the pulse plating was quite long. Typically, these pulses should have been in the millisecond range. A power supply capable of these short pulses was ordered, but did not arrive in time to affect the program.

The chloride system may be another system to explore. The $ZrCl_4$ will still react with the uranium to form UF_3, but the delta G of reaction (see Figure 5.3) is lower than in the fluoride system, and correspondingly, the voltage needed to prevent the reaction is lower. However, this system was not pursued because, in the literature, it proved difficult to produce coherent plates; there was also no prior experience with the system at PNNL.
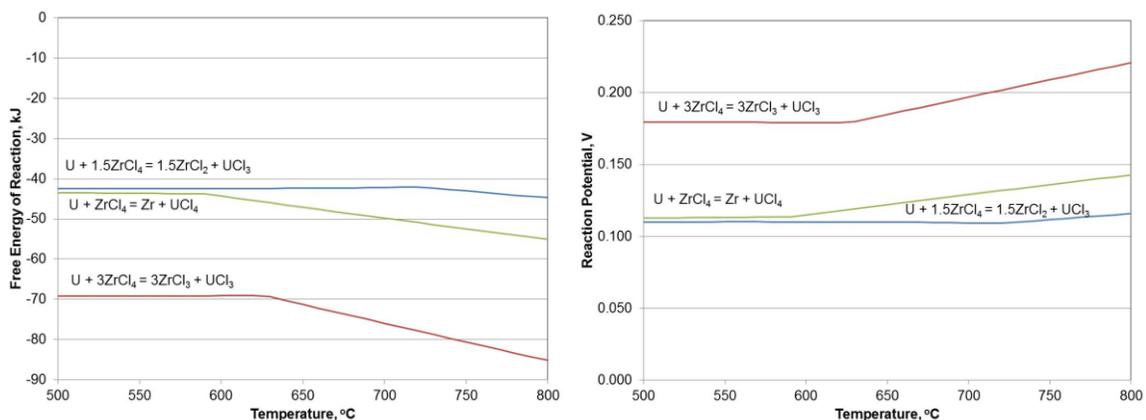
Figure 5.3. Cell Potentials and Reaction Energies for Displacement Reactions in Chloride System

5.2

6.0   Conclusions

During the course of this effort, the following conclusions were made:

- The formation of UF_x must be suppressed to form an adequate plating. The UF_x will spontaneously form in the ZrF_4-containing salt bath, and must be prevented by applying a cathodic potential of greater than 0.4 V.

- Platings were successfully made on homogenized U-10Mo samples with an applied terminal potential of 2 V in a bath of $NaF:LiF:ZrF_4$. The zirconium-plated layer had excessive dendritic growth.

- Plating above 700°C resulted in rapid formation of Mo_2Zr intermetallics. Plating should be carried out below 650°C, or be of a sufficiently short duration to minimize the interaction.

- Homogenization of the U-10Mo had an impact on the formation of UF_x. Unhomogenized U-10Mo was not plated with any conditions in a ZrF_4-containing bath.

- For bath compositions containing ZrF_4, good coherent plates were achieved only when terminal voltages were greater than 1 V. However, these high voltages also produce dendritic growth.

- ZrF_4 is not needed in a bath composition to produce plating.

7.0   References

Basile F, E Chassaing, and G Lorthioir. 1981. "Electrochemical reduction of $ZrCl_4$ in molten NaCl, CsCl and KCl-LiCl and chemical reactions coupled to the electrodeposition of zirconium." *Journal of Applied Electrochemistry* 11(5):645−651.23108

Coffey GW, VV Joshi, LR Pederson, CA Lavender, DM Paxton, and D Burkes. 2014. *Concept Feasibility Report for Electroplating Zirconium onto Molybdenum Foil*. PNNL-23108, Pacific Northwest National Laboratory, Richland, Washington. [Limited Distribution]

Flengas SN, JE Dutrizac, and RL Lister. 1968. "Properties of the solutions of the alkali-chlorozirconate compounds in alkali-chloride melts." *Canadian Journal of Chemistry* 46(4):495−502.

Girginov A, TZ Tzvetkoff, and M Bojinov. 1995. "Electrodeposition of refractory metals (Ti, Zr, Nb, Ta) from molten salt electrolytes." *Journal of Applied Electrochemistry* 25(11):993−1003.

Groult H, A Barhoun, H El Ghallali, S Borensztjan, and F Lantelme. 2008. "Study of the Electrochemical Reduction of Zr^{4+} Ions in Molten Alkali Fluorides." *Journal of the Electrochemical Society* 155(2):E19-E25.

Groult H, A Barhoun, E Briot, F Lantelme, and CM Julien. 2011. "Electrodeposition of Zr on graphite in molten fluorides." *Journal of Fluorine Chemistry* 132(12):1122−1126.

Guang-Sen C, M Okido, and T Oki. 1990. "Electrochemical studies of zirconium and hafnium in alkali chloride and alkali fluoride-chloride molten salts." *Journal of Applied Electrochemistry,* 20(1):77−84.

Kipouros GJ and SN Flengas. 1985. "Electrorefining of Zirconium Metal in Alkali Chloride and Alkali Fluoride Fused Electrolytes." *Journal of the Electrochemical Society* 132(5):1087−1098.

Lister RL and SN Flengas. 1965. "On the Relationship Between Equilibrium Pressures and the Phase Diagram of a Reactive System, the Systems: $NaCl-Na_2ZrCl_6$, $KCl-K_2ZrCl_6$, $NaCl-KCl-ZrCl_4$." *Canadian Journal of Chemistry* 43(11):2947−2969.

Malyshev V, A Gab, A Izvarina, AM Popescu, and V Constantin. 2010. "Electroreduction of Potassium Fluorozirconate on the Background of Chloride and Chloride-Fluoride Melts." *Revue Roumaine De Chimie* 55(3):179−185.

Mellors GW and S Senderoff. 1965. "The Electrodeposition of Coherent Deposits of Refractory Metals, I.Zirconium." *Journal of the Electrochemical Society* 112(3):266−272

Mellors GW and S Senderoff. 1966. "The Electrodeposition of Coherent Deposits of Refractory Metals, III.Zirconium." *Journal of the Electrochemical Society* 113(1):60−66.

Nissen DA and RW Stromatt. 1968. *Zirconium Electroplating on Uranium from Molten Alkali Fluoride Salts*. BNWL-825, Battelle Pacific-Northwest Laboratories, Richland, Washington.

Sakamura Y. 2004. "Zirconium Behavior in Molten LiCl-KCl Eutectic." *Journal of the Electrochemical Society* 151(3):C187−C193.

Salannea M, C Simon, H Goult, F Lantelme, T Goto, and A Barhoun. 2009. "Transport in molten LiF–NaF–ZrF$_4$ mixtures: A combined computational and experimental approach." *Journal of Fluorine Chemistry* 130(1):61−66.

Senderoff S and GW Mellors. 1966. "Coherent Coatings of Refractory Metals." *Science* 153(3743):1475−1481.

Distribution

No. of
Copies

1   Department of Energy National Nuclear
    Security Administration
    Global Threat Reduction Initiative
    1000 Independence Ave.
    Washington, DC 20002
        Mr. Christopher Landers
        Mr. Bryan Reed

1   Idaho National Laboratory
    P.O. Box 1625
    Idaho Falls, ID 83415
        Mr. Kenneth Rosenberg
        Dr. Mitchell Meyer

1   Argonne National Laboratory
    9700 S Cass Ave.
    Argonne, IL 60439
        Dr. Eric Wilson

2   **Local Distribution**

    Pacific Northwest National Laboratory
    Greg Coffey   PDF
    Kerry Meinhardt   PDF
    Vineet Joshi   PDF
    Larry Pederson   PDF
    Curt Lavender   Mail Stop K2-44
    Douglas Burkes   Mail Stop K8-34